JTTEE5 8:323-327

Temperature Measurements and Adhesion Properties of Plasma Sprayed Thermal Barrier Coatings

C.R.C. Lima and R. da Exaltação Trevisan

(Submitted 15 August 1998; in revised form 8 January 1999)

Metal-ceramic coatings have been widely used for industrial applications, mainly in the gas turbine and diesel engine industries as thermal barrier coatings (TBCs). Conventional thermal barrier coatings consist of a metallic bond coat and an insulating ceramic topcoat. Temperatures and temperature gradients in the coating during plasma spraying play an important role on the final coating quality, especially the temperature of the particles just hitting the substrate surface. In this work, metal-ceramic coatings were applied on nickel-superalloy substrates. The temperatures of both the coating surface and substrate were measured during spraying. The adhesion of the coatings was determined using ASTM C 633 and correlated with the measured temperatures. Optical pyrometry and thermocouples were used to measure the interfacial and substrate temperatures, respectively. Temperature was shown to have a significant influence where lower interfacial temperatures were found to result in lower adhesion values.

Keywords adhesion, temperature influence, thermal barrier coatings

1. Introduction

Thermal barrier coatings (TBC) have been used to protect metallic components, which are subject to corrosion, oxidation, or excessive heating during service in thermal environments. Conventional TBCs are composed of a metallic bond coat over a metallic substrate and an insulating ceramic top coating (Ref 1). This system presents stresses, which are generated during or after spraying and are detrimental to the quality of the coatings (Ref 2). At the metallic bond coat/ceramic topcoat interface this fact is aggravated due to the mismatch of the thermal expansion coefficients of the metal and ceramic. Several studies have been carried out in an attempt to overcome this restriction (Ref 3-7). Functional gradient coatings (FGM) have been developed to solve the problems associated with early spallation of plasma sprayed TBCs and other metal-ceramic systems (Ref 8-12). Temperatures and temperature gradients in the coatings during plasma spraying have a strong influence on the coating quality, especially the temperature and velocity of the particles impacting the substrate surface. The temperatures are generated by the plasma beam, which contains hot gases and molten particles. Thermal energy from the molten or semimolten particles is induced into the substrate and coating, which as a result affects the thermophysical, chemical, and mechanical properties (Ref 13, 14). Cooling is generally applied to reduce the thermal load on the materials.

C.R.C. Lima, UNIMEP, Methodist University of Piracicaba,Technology Center, Rod. Santa Bárbara, Iracemápolis, Km 1 Santa Bárbara d'Oeste, Sao Paulo, Brazil 13450-000; and **R. da Exaltação Trevisan,** UNICAMP, State University of Campinas, College of Mechanical Engineering, Campinas, Sao Paulo, Brazil. Contact e-mail: crclima@unimep.br.

In this study, metallic and ceramic coatings were sprayed, using atmospheric plasma spraying (APS), on nickel-superalloy substrates. Temperatures reached at the coating surface and substrate were measured during spraying to study the influence of temperature on the coating characteristics and adhesion properties. Coatings with a conventional metallic bond coat and with a mixed metal-ceramic bond coat were applied for further comparison. The interfacial temperature measurements were performed by optical pyrometry. The substrate temperature was measured by thermocouples positioned at the back face of the substrates. The phase content of the coatings was evaluated by x-ray diffraction. The adhesion of the coatings was evaluated using ASTM C 633 (Ref 15).

2. Experimental Procedure

Nickel superalloy (Inconel 718) was used as the substrate material. For the coating, a metallic Ni-Cr-Al alloy powder (–120 to +45 μm) and a ZrO_2-8wt%Y_2O_3 (–75 to +45 μm) powder were used (Table 1). Three types of bond coat were prepared: 100 wt% metallic, 50 wt% metallic/50 wt% ceramic, and 25 wt% metallic/75 wt% ceramic. The powders of the metal-ceramic mixed bond coats were premixed (mechanically) before feeding. Both powders were chosen for compatible particle size in order to have powder mixture homogeneity before and during thermal spraying. A "Latin square" design (Ref 16) was applied for three levels and two variability parameters: thickness and quantity of layers, where "layer" refers to different metal-ceramic composition of the coating. A ceramic layer was always deposited over the bond coat. Experiments were performed for samples with only the bond coat layer as well as with the complete coating (i.e., bond coat and ceramic top coat). A 7MC-II plasma spray system was used for the spraying process equipped with a 6MP (Metco Code No.) dual feeder and a 9MB spray gun (Metco, Westbury, NY). Table 2 summarizes deposition parameters for

the plasma spray protocol. The test specimens (25 mm in diameter and 25 mm in thickness) were grit blasted shortly before spraying. The tensile adhesion measurements were performed according to ASTM C 633-79 (Ref 15). The adhesive bonding agent used was a two-part, epoxy-based mix, which cured at room temperature (DP-460, 3M, São Paulo, Brazil).

Temperatures at the interfaces were measured using optical pyrometry (Pirograf-IS-2-SP pyrometer, RenéGraf, São Paulo, Brazil) with a temperature measuring range of 900 to 3000 °C. Substrate temperature measurements were carried out using a "K" type thermocouple (0.1 mm diameter), with the thermocouples welded on the rear face of test specimens. The difficulties in registering temperatures at the interfaces are well known, mainly due to the dynamic nature of the coating during spraying. Several authors have tried "online" measurements to correlate registered and calculated values and their influence on the coating properties (Ref 13, 17, 18, 19). The complete description of the temperature measurement and data acquisition system used in this experiment can be found in Ref 20.

X-ray diffraction was carried out using a Rigaku Geigerflex diffractometer (Rigaky, Tokyo, Japan), with an Analyx type A 41L-Cu tube working at 60 kV to 20 kW. The measurement voltage was 30 kV, and the beam amperage was 15 mA for a 2θ scanning of 10 to 90° with maximum counting of 5 kcps. The measurements were performed for all coated samples as well as for the as-received metal and ceramic powders.

Table 1 Chemical analysis of materials

Element	Composition, wt%
Inconel 718	
C	0.03
Si	0.07
Cr	17.76
Mo	3.05
Ni	bal
Ti	1.07
Nb	5.12
Al	0.57
Fe	18.8
Metallic powder	
Ni-Cr blend	94.00
Al	6.00
Ceramic powder	
ZrO_2	92.00
Y_2O_3	8.00

Table 2 Plasma spray parameters

Arc voltage, V	60-70
Arc current, A	500
Arc gas	Argon-hydrogen
Argon flow rate, L/min	80
H_2 flow rate, L/min	15
Spray distance, mm	80
Deposition rate, kg/h	1.1
Argon carrier gas flow rate, L/min	37
Transverse speed, mm/s	100

Table 3 Tensile adhesion test results for mixed 25% metallic/75% ceramic bond coat specimens

Test specimen	Thickness, μm	Adhesion strength, MPa	Fracture pattern analysis
09	70	19.5	Adhesive, 80% substrate-bond coat interface
12	300	14.0	Adhesive, 55% substrate-bond coat interface
16	150	31.3	Adhesive, 60% substrate-bond coat interface
18	500	16.8	Cohesive, 55% bond coat-ceramic coat
22	350	12.7	Cohesive, 70% bond coat
23	700	11.7	Mixed, 40% substrate bond coat interface/40% bond coat

3. Results and Discussion

The tensile adhesion test results are listed in Tables 3 to 5 for the different bond coat series. The fracture pattern analysis is included in the same tables, showing the percentage of adhesive or cohesive fracture. The analysis was done using an image analysis software MOCHA (Jandel Scientific, São Paulo, Brazil). The tensile strength of a thermal spray coating consists of the bonding between the coating and the substrate (adhesive strength) and the bonding between the particles within the coating (cohesive strength). Fracture during the tensile adhesion test can occur completely at the coating/substrate interface, completely in the coating, or in a mixed way, that is, partially in the coating and partially at the coating/substrate interface. These fracture patterns characterize adhesive fracture, cohesive fracture, or mixed adhesive/cohesive fracture, respectively (Ref 21).

Results from the temperature measurements are listed in Tables 6 and 7, measured using a pyrometer and a thermocouple, respectively. Some values were not registered due to the interference with the high frequency plasma equipment. The results from Tables 6 and 7 are also presented in Fig. 1. Table 8 summarizes the x-ray diffraction results of the coatings. The most intense peaks from the elements or phases are first presented followed by the less intense peaks. X-ray analysis of the as-received powders is also included as a reference. Tetragonal nontransformable zirconia (t′) was the predominant phase for all the ceramic coatings, regardless of the coatings structure.

It can be observed from Fig. 1, for the group of coatings with a 25% metallic/75% ceramic bond coat, that temperature in the

Table 4 Tensile adhesion test results for mixed 50% metallic/50% ceramic bond coat specimens

Test specimen	Thickness, μm	Adhesion strength, MPa	Fracture pattern analysis
01	200	20.8	Adhesive, 90% substrate-bond coat interface
04	700	8.8	Adhesive, 60% substrate-bond coat interface
19	100	12.5	Adhesive, 80% substrate-bond coat interface
21	300	13.5	Cohesive, 55% ceramic coat
24	250	17.9	Adhesive, 70% substrate-bond coat interface
25	500	19.4	Adhesive, 70% substrate-bond coat interface

coating formation surface tends to decrease as the coating thickness increases. This can be explained by the increase in the amount of ceramic content for a specific coating. This behavior was also observed for temperatures measured by the thermocouples (Fig. 1). The phase distribution analysis (Table 8) indicates a higher presence of zirconia for the groups of coatings with mixed bond coats.

Temperatures measured using thermocouples for test specimens with 25 wt% metallic/75 wt% ceramic bond coat were lower than that measured from the group with 50 wt% metallic/50 wt% ceramic bond coat, regardless of the coating thickness (Fig. 1). Test specimens TS 9 and TS 19, for instance, which are representative of the two groups of mixed bond coats, showed quite similar composition analysis for metallic and ceramic phases. Adhesion values for the same specimens were higher for the 25 wt% metallic/75 wt% ceramic group (19.5 MPa for TS 9, for example) than for the 50 wt% metallic/50 wt% ceramic group (12.5 MPa for TS 19). It should also be noted that both specimens presented similar fracture patterns. Higher temperatures measured using the pyrometer compared to lower temperatures measured using the thermocouple indicated lower heat dissipation from the coating-substrate interface, leading to higher interfacial temperature and hence better adhesion. The interfacial temperature was characterized by the contact temperature at the particle-substrate boundary during the impact of the sprayed powder. This temperature markedly influenced the adhesion of the sprayed coating to the substrate. Increasing the contact temperature between the particles and the substrate resulted in an increase in the number of contact zones due to better spreading of the molten particles and consequently improvement in the adhesion of the coating to the substrate either for metals or ceramics (Ref 22, 23). Furthermore, some studies of coating formation during plasma spraying of molybdenum have concluded that with increasing the contact temperature, the coating exhibits better lamellar structure with less interlamellar pores and debris, resulting in better adhesion and bonding of the splats (Ref 24).

Table 5 Tensile adhesion test results for 100% metallic bond coat specimens

Test specimen	Thickness, μm	Adhesion strength, MPa	Fracture pattern analysis
05	125	33.8	Adhesive, 70% substrate-bond coat interface
08	500	16.6	Cohesive, 55% ceramic coat
13	250	18.2	Not valid, failure in the epoxy adhesive
15	700	30.4	Cohesive, 80% bond coat-ceramic coat
26	150	38.7	Adhesive, 60% substrate-bond coat interface
27	300	36.1	Adhesive, 60% substrate-bond coat interface

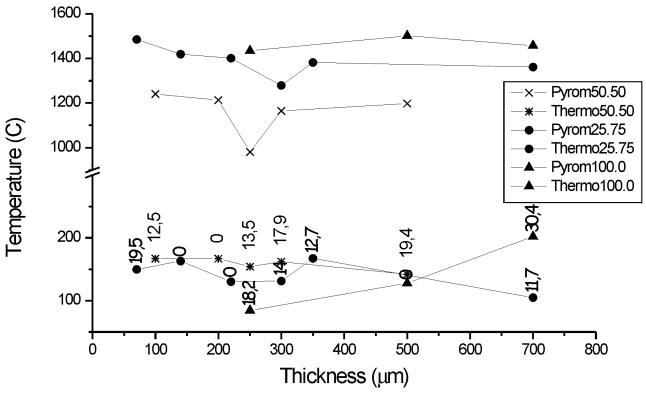

Fig. 1 Graphic of the temperatures for the three different bond coat series. The adhesion values from Table 6 are presented as labels over the thermocouple lines.

Table 6 Temperature measurements using a pyrometer

Test specimen	Thickness, μm	Average temperature, °C	Standard deviation	Adhesion strength, MPa
25% metallic/75% ceramic bond coat				
09	70	1484.8	128.4	19.5
10	140	1419.3	147.9	NR
11	220	1401.5	162.9	NR
12	300	1279.5	115.2	14.0
22	350	1382.2	112.2	12.7
23	700	1361.3	190.7	11.7
50% metallic/50% ceramic bond coat				
19	100	1240.0	255.5	12.5
20	200	1213.5	141.8	NR
21	300	1165.3	135.9	13.5
24	250	980.6	104.4	17.9
25	500	1198.2	166.8	19.4
100% metallic bond coat				
13	250	1434.3	173.6	18.2
14	500	1501.1	266.3	NR
15	700	1456.8	254.8	30.4

NR, value not registered

Table 7 Temperature measurements using thermocouple

Test specimen	Thickness, μm	Average temperature, °C	Standard deviation	Adhesion strength, MPa
25% metallic/75% ceramic bond coat				
09	70	149.6	50.3	19.5
10	140	162.8	44.4	NR
11	220	130.0	41.7	NR
12	300	131.4	40.8	14.0
22	350	167.2	44.3	12.7
23	700	104.6	34.3	11.7
50% metallic/50% ceramic bond coat				
19	100	166.8	51.4	12.5
20	200	166.8	38.5	NR
21	300	162.1	40.7	13.5
24	250	154.1	39.9	17.9
25	500	141.9	65.8	19.4
100% metallic bond coat				
13	250	84.1	46.1	18.2
14	500	127.9	59.3	NR
15	700	202.2	55.3	30.4

NR, value not registered

The temperatures measured by the pyrometer for the group with 100% metallic bond coat were the highest, while the temperatures measured by thermocouples were the lowest, which agrees with the previous discussion. In general, the tensile adhesion test (TAT) results were higher for this group compared with the other groups (Fig. 1). Even for TS 15, which indicated a high temperature read by the thermocouple (202 °C), the adhesion value was high (30.4 MPa). Lower adhesion values, such as 18.2 MPa for TS 13 in Table 5, refer to an unacceptable adhesion test where the failure occurred at the adhesive agent, not at the coating. Figures 2 and 3 are characteristics of the thermal profile recorded during spraying (first pass) of the metal and metal-ceramic bond coat series, respectively. Thermal profile analysis of such data show that the pyrometer measures the temperature at the time when the particles contact the substrate. A better temperature stability was present for the completely metallic bond coated test specimens compared to the metallic-ceramic bond coat mixture test specimens. This can be correlated with the presence of a homogeneous temperature distribution for the metallic bond coat samples, while the temperature distribution is disturbed with the inclusion of ceramic particles in the metal-ceramic, bond-coated samples.

It should be noted that in the tensile adhesion tests, the adhesion was calculated by dividing the maximum load by the tested cross-sectional area. This means that the practical adhesion was measured (Ref 25). According to some authors, the basic adhesion or the true adhesion should be evaluated considering, in the case of partial failure, the part of the coating that remains on the substrate after the test, which is intact and did not detach or fail. That remaining coating should be tested again in order to obtain the adhesion of the complete coating (Ref 25, 26). The temperatures ranked in Tables 6 and 7 are averages for the complete coatings. Hence, the interfacial temperature influence on the coating formation needs to be considered. Therefore the intent of substrate preheating by some authors (Ref 27) is for the same impact particles to impact under the same thermal conditions during the entire time of the thermal spray process.

Table 8 Distribution of phases results from x-ray diffraction

Test specimen	Thickness, μm	Elements/phases components → (direction of lower peak intensity) →						
Metallic powder	…	Cr	Ni	Al	…	…	…	…
Ceramic powder	…	ZrO_2(T)	ZrO_2(M)	Y_2O_3	…	…	…	…
Metal ceramic mixture 100%M-0%C								
05	125	Cr	Ni	…	…	…	…	…
08	500	ZrO_2(T)	ZrO_2(C)	ZrO_2(M)	…	…	…	…
13	250	Cr	Ni	…	…	…	…	…
15	700	ZrO_2(T)	ZrO_2(C)	ZrO_2(M)	…	…	…	…
26	150	Cr	Ni	…	…	…	…	…
27	300	ZrO_2(T)	ZrO_2(C)	ZrO_2(M)	Y_2O_3	ZrO	…	…
Metal ceramic mixture 50%M-50%C								
01	200	ZrO_2(T)	Cr	Ni	ZrO_2(C)	ZrO_2(M)	AlNi	Y_2O_3
04	700	ZrO_2(T)	ZrO_2(C)	ZrO_2(M)	…	…	…	…
19	100	ZrO_2(T)	Cr	$NiCrO_3$	AlNi	…	…	…
21	300	ZrO_2(T)	ZrO_2(C)	…	…	…	…	…
24	250	ZrO_2(T)	Cr	ZrO_2(C)	Ni	AlNi	…	…
25	500	ZrO_2(T)	ZrO_2(C)	…	…	…	…	…
Metal ceramic mixture 25%M-75%C								
09	70	ZrO_2(T)	Al_3Ni	Cr	Zr_3O	…	…	…
12	300	ZrO_2(T)	ZrO_2(C)	ZrO_2(M)	…	…	…	…
16	150	ZrO_2(T)	Ni	Al_2Cr	ZrO_2(C)	Cr	ZrO_2(M)	…
18	500	ZrO_2(T)	ZrO_2(C)	ZrO_2(M)	…	…	…	…
22	350	Cr	ZrO_2(T)	ZrO_2(M)	ZrO_2(C)	Ni	Al_2Cr	…
23	700	ZrO_2(T)	ZrO_2(C)	…	…	…	…	…

T, tetragonal nontransformable; C, cubic; M, monoclinic

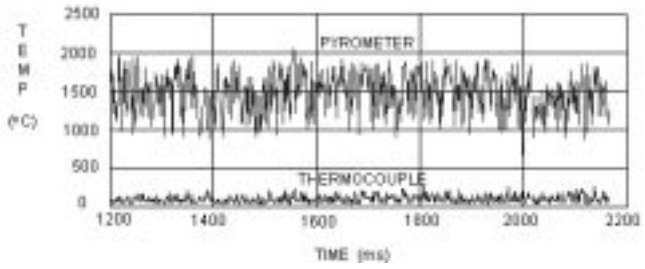

Fig. 2 First pass temperatures for test specimen with metallic bond coat

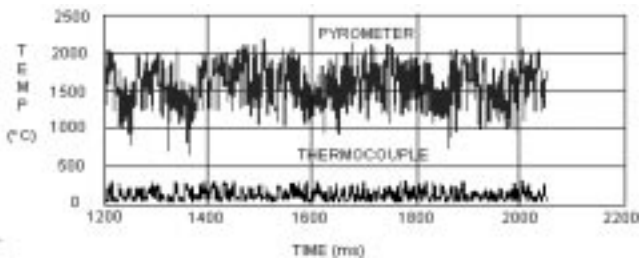

Fig. 3 First pass temperatures for test specimen with metal-ceramic bond coat

4. Conclusions

The following conclusions are based on this work:

- The 100% metal coatings present higher thermal stability at the measured interface compared to the metal-ceramic coatings (25 wt% metallic/75 wt% ceramic or 50 wt% metallic/50 wt% ceramic), thus leading to higher adhesion values.
- Higher interfacial temperature leads to higher adhesion strength, regardless of the metal-ceramic composition of the coatings.
- Tetragonal nontransformable (t′) zirconia was the predominant phase for all the ceramic coatings, regardless of the coating structure.

Acknowledgments

The authors acknowledge Rolls Royce Motors, Brazil, for technical collaboration and FAPESP, São Paulo, Brazil, for financial support.

References

1. M.L. Thorpe, Major Advances Noted in Thermal Spray Technology, *Adv. Mater. Process.*, Vol 1, 1993, p 23-24
2. L. Pawlowski, *The Science and Engineering of Thermal Spray Coatings*, John Wiley & Sons, 1995
3. W. Smith, T.J. Jewett, S. Sampath, C.C. Berndt, H. Herman, J. Fincke, and R.N. Wright, Plasma Processing of Functionally Graded Materials: Diagnostics and Characterization, *Thermal Spray: Practical Solutions for Engineering Problems*, C.C. Berndt, Ed., ASM International, 1996, p 317-324
4. T. Cosack, L. Pawlowski, S. Schineiderbanger, and S. Sturlese, Thermal Barrier Coatings on Turbines Blades by Plasma Spraying with Improved Cooling, *J. Eng. Gas Turbines Power (Trans. ASME)*, Vol 116, 1991, p 272-276
5. H.L. Tsai and P.C. Tsai, Performance of Laser-Glazed Plasma Sprayed (ZrO_2-12wt%Y_2O_3)/(Ni-22wt%Cr-10wt%Al-1wt%Y) Thermal Barrier Coatings in Cyclic Oxidation Tests, *Surf. Coat. Technol.*, Vol 71, 1995, p 53-59
6. K. Suganuma, Y. Myiamoto, and M. Koizumi, Joining of Ceramic and Metals, *Ann. Rev. Mater. Sci.*, Vol 18, 1988, p 47-73
7. D.J. Greving, J.R. Shadley, and E.F. Rybicki, Effects of Coating Thickness and Residual Stresses on Bond Strength of C-633-79 Thermal Spray Coating Test Specimen, *Thermal Spray Industrial Applications*, C.C. Berndt and S. Sampath, Ed., ASM International, 1994, p 639-645
8. J.T. Demasi-Marcin and D.K. Gupta, Protective Coatings in the Gas Turbine Engine, *Surf. Coat. Technol.*, Vol 68/69, 1994, p 1-9
9. K.G. Schimitt-Thomas and U. Dietl, Thermal Barrier Coatings with Improved Oxidation Resistance, *Surf. Coat. Technol.*, Vol 68/69, 1994, p 113-115
10. Y.C. Tsuy and T.W. Cline, Adhesion of Thermal Barrier Coating Systems and Incorporation of an Oxidation Barrier Layer, *Thermal Spray: Practical Solutions for Engineering Problems*, C.C. Berndt, Ed., ASM International, 1996, p 275-284
11. W.J. Brindley, Properties of Plasma-Sprayed Bond Coats, *J. Therm. Spray Technol.*, Vol 6 (No. 1), 1997, p 85-90
12. M.R. Dorfman, B.A. Kushner, and A.J. Rotolico, *A Review of Thermal Barrier Coatings for Diesel Engines Applications*, Metco/Perkin Helmer Int. Com., 1991, p 1-19
13. H.J. Sölter, U. Muller, and E. Lugscheider, High-Speed Temperature Measurement for On-Line Process Control and Quality Assurance during Plasma Spraying, *Powder Metall. Int.*, Vol 24 (No. 3), 1992, p 169-174
14. P. Scardi, E. Galvanetto, A. Tomasi, and L. Bertamini, Thermal Stability of Stabilized Zirconia Thermal Barrier Coatings Prepared by Atmosphere- and Temperature-Controlled Spraying, *Surf. Coat. Technol.*, Vol 68/69, 1994, p 106-112
15. "Standard Method of Test for Adhesion or Cohesive Strength of Flame Sprayed Coatings," C 633, *19th Annual Book of ASTM Standards*, Part 17, ASTM, 1979, p 636-642
16. R.V. Hogg and J. Ledolter, *Applied Statistics for Engineers and Physical Scientists*, Macmillan, 1992
17. C.P. Bergman, Plasma Deposition of Ceramic Layers: Part I: Interfacial Temperature Measurement during Process, *Cerâmica*, Vol 39 (No. 260), 1993, p 17-20 (in Portuguese)
18. L. Pawlowski, M. Vardelle, and P. Fauchais, A Model of the Temperature Distribution in an Alumina Coating during Plasma Spraying, *Thin Solid Films*, Vol 94, 1982, p 307-319
19. M.K. Hobbs and H. Reiter, Residual Stresses in ZrO_2-8%Y_2O_3 Plasma Sprayed Thermal Barrier Coatings, *Surf. Coat. Technol.*, Vol 34, 1988, p 33-42
20. C.R.C. Lima and R.E. Trevisan, Influence of Interfacial Temperature on the Adhesion Properties of Plasma Sprayed Metal-Ceramic Coatings, *Thermal Spray: Meeting the Challenges of the 21st Century*, Vol 2, C. Coddet, Ed., ASM International, 1998, p 1555-1560
21. *Thermal Spraying-Practice, Theory and Applications*, American Welding Society, Miami, 1985
22. L. Pawlowski, Temperature Distribution in Plasma-Sprayed Coatings, *Thin Solid Films*, Vol 81, 1981, p 79-88
23. H.D. Steffens, B. Wielage, and J. Drozak, Interface Phenomena and Bonding Mechanism of Thermally-Sprayed Metal and Ceramic Composites, *Surf. Coat. Technol.*, Vol 45 (No. 1-3), 1991, p 299-308
24. X.Y. Jiang, S. Sampath, A. Vardelle, M. Vardelle, and P. Fauchais, Microstructure Development during Plasma Spraying of Molybdenum Part 2: Coating Microstructure and Properties, *Thermal Spray: Meeting the Challenges of the 21st Century*, Vol 2, C. Coddet, Ed., ASM International, 1998, p 735-740
25. K.L. Mittal, Adhesion Measurement: Recent Progress, Unsolved Problems and Prospects, *ASTM Special Tech. Publications 640*, ASTM, 1978, p 5-17
26. H.D. Steffens, B. Wielage, and J. Drozak, Interface Phenomena and Bonding Mechanism of Thermally Sprayed Metal and Ceramic Composites, *Surf. Coat. Technol.*, Vol 45, 1991, p 299-308
27. A. Haddadi, A. Grimaud, A. Denoirjean, F. Nardou, and P. Fauchais, Crystalline Growth within Alumina and Zirconia Coatings with Coating Temperature Control during Spraying, *Thermal Spray: Practical Solutions for Engineering Problems*, C.C. Berndt, Ed., ASM International, 1996, p 615-622